Top Catal (2007) 46:306–319
DOI 10.1007/s11244-007-9004-9

ORIGINAL PAPER

First Principles Analysis of the Electrocatalytic Oxidation of Methanol and Carbon Monoxide

Michael J. Janik · Christopher D. Taylor · Matthew Neurock

Published online: 27 November 2007

Abstract The strong drive to commercialize fuel cells for portable as well as transportation power sources has led to the tremendous growth in fundamental research aimed at elucidating the catalytic paths and kinetics that govern the electrode performance of proton exchange membrane (PEM) fuel cells. Advances in theory over the past decade coupled with the exponential increases in computational speed and memory have enabled theory to become an invaluable partner in elucidating the surface chemistry that controls different catalytic systems. Despite the significant advances in modeling vapor-phase catalytic systems, the widespread use of first principle theoretical calculations in the analysis of electrocatalytic systems has been rather limited due to the complex electrochemical environment. Herein, we describe the development and application of a first-principles-based approach termed the *double reference method* that can be used to simulate chemistry at an electrified interface. The simulations mimic the half-cell analysis that is currently used to evaluate electrochemical systems experimentally where the potential is set via an external potentiostat. We use this approach to simulate the potential dependence of elementary reaction energies and activation barriers for different electrocatalytic reactions important for the anode of the direct methanol fuel cell. More specifically we examine the potential-dependence for the activation of water and the oxidation of methanol and CO over model Pt and Pt alloy surfaces. The insights from these model systems are subsequently used to test alternative compositions for the development of improved catalytic materials for the anode of the direct methanol fuel cell.

Keywords Electrocatalysis · DFT · First principles · Ab initio · DMFC · PEMFC

M. J. Janik
Department of Chemical Engineering, The Pennsylvania State University, 104 Fenske Laboratory, University Park, PA 16802, USA

C. D. Taylor
Materials Science and Technology, Los Alamos National Laboratory, Los Alamos, NM, USA

M. Neurock (✉)
Department of Chemical Engineering and Chemistry, University of Virginia, 102 Engineers' Way, Charlottesville, VA 22904, USA
e-mail: mn4n@virginia.edu

1 Introduction

The increased drive to create more efficient, portable, and flexible energy conversion technologies has led to a tremendous increase in research aimed at the design and development of active electrocatalysts for both the anode and the cathode of proton exchange membrane (PEM) based fuel cells [1–5]. PEM fuel cell efficiencies and power outputs have been limited by the achievable reaction rates and overpotentials associated with both electrodes. For example, 20–35% of cell fuel efficiency in a PEM fuel cell is sacrificed to create an overpotential to drive oxygen reduction at a platinum cathode [6]. Anode inefficiencies further limit the performance of direct methanol fuel cells [5, 7]. Furthermore, state-of-the-art electrodes for these reactions contain significant amounts of platinum which contributes to high overall costs [5]. Experimental research has furthered our understanding of fundamental electrode processes and improved the design of fuel cell electrodes, with techniques ranging from membrane/electrode assembly testing and characterization [6, 8], single electrode

electrochemical reactivity studies [7, 9–12], and fundamental surface characterization [13–15].

Ab initio quantum mechanical (QM) methods can complement these fundamental efforts but have traditionally been limited by their ability to capture the complex catalytic and electrochemical environments. The tremendous advances that have taken place over the past decade in the application of theory to understanding the surface reactivity of more traditional vapor-phase catalytic systems, however, has made it an invaluable partner in elucidating catalytic reaction mechanisms and aiding the design of new catalytic materials. This success has fueled recent computational efforts in examining electrochemical systems. Much of this work, however, has focused on understanding the catalytic paths in idealized environments. The complexities of the electrified water/metal interface have been either ignored or treated in a cursory fashion.

The complexity of the electrified solution metal interface is highlighted in the schematic shown in Fig. 1. The ability to model electrochemical and electrocatalytic systems requires treating many of the same issues present in more traditional heterogeneous vapor phase catalytic systems including: (1) metal/support interactions, (2) particle size and morphological effects, (3) the influence of surface coverage, (4) the addition of an alloying metal, and (5) promoter or poison effects. In addition, there are a host of complexities that result from the electrochemical environment which include the influence of solution, electrolyte, applied potentials or electric fields and electron transfer. This degree of complexity has historically limited the application of theory to modeling electrochemical and electrocatalytic systems.

The reaction energies and activation barriers associated with elementary kinetic processes determined using QM methods along with transition state theory are typically based on a canonical formalism whereby the number of electrons and nuclei remain constant between the reactant and product systems. The kinetics for electron and proton transport between "compartments" within the fuel cell, however, are intrinsic to the overall function of the device, thus the use of a model system where the number of electrons and nuclei are intrinsically conserved requires the simultaneous consideration of the anode, membrane, and cathode within the QM model system. For example, if we wish to simulate the kinetics of an oxidation reaction step at the anode of a proton-exchange membrane fuel cell (PEMFC), the calculation of comparable reactant and product energies is complicated by the fact that the proton and electron product energies are not correctly represented if they reside in the same model system as the reactant. The challenge toward simulating electrochemical systems then is to define a model system that appropriately represents the interactions at a single electrode while also providing

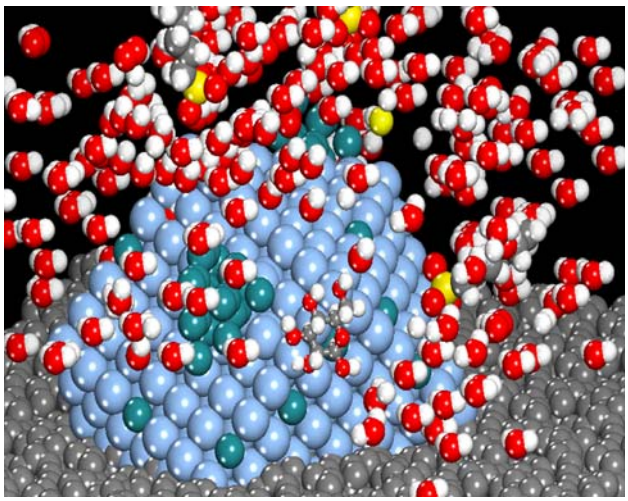

Fig. 1 Illustration of the reaction environment about an electrocatalyst. A Pt–Ru bimetallic particle is supported on a high surface area, electron conducting support. Reaction occurs on the bimetallic surface in the presence of solution and charge-compensating electrolyte. The electric field at the particle surface may affect the rate of an elementary reaction step, such as the coupling of adsorbed CO and OH species leading to CO_2 production. Carbon atoms in gray represent the electron conducting support and polymer backbone. Pt and Ru atoms with light and dark blue, O atoms are red, S atoms are yellow, and white spheres represent hydrogen

for the consideration of the elementary processes that, for an oxidation step, produce electrons and ions that complete the reaction step in a different environment.

Within even the half-cell environment, simulating the electrocatalytic performance of a fuel cell anode would require consideration of the complex environment presented in Fig. 1. Such an approach is well beyond what is feasible today or likely over the next decade using QM methods. Even if we had the ability to do so, including all complexities in the model system makes it difficult to differentiate how various factors influence the electrocatalytic performance. Much more can be learned by systematically varying the features of idealized systems and subsequently increasing the complexity in the system. Herein, model single crystal substrates are used to represent the electrode surface. A large ensemble of explicit water molecules at the appropriate density is incorporated near the surface to represent the solution phase. The influence of electrochemical potential at the interface is examined using an approach we recently developed, which is reviewed in the methods section. The presence of electrolyte and the electric field that develops across the electrochemical double layer will significantly influence elementary reaction energetics occurring at the metal interface, and cannot easily be discarded from the QM model system. The binding of different adsorbates to the electrodes is significantly affected by the electrode potential, the interfacial electric field, and the presence of

electrolyte at the interface. Quantitative modeling of the potential dependence of this interaction is needed to further understanding of the fundamental kinetic processes that occur at the electrode surface. The introduction of a variable electrode potential and interfacial potential drop in the model system is necessary to understand the potential dependence of electrocatalytic reaction rates. Finally, in moving from reactants to products, the electrode potential must remain constant in order to simulate electrochemical or electrocatalytic behavior. The production of electrons by elementary oxidation reaction steps will alter the electrode potential if they are allowed to remain within the model system in the product state.

A number of elementary interactions that would be present in the anode environment of a fuel cell are neglected in order to directly probe the effects of solution and electrode potential on elementary reaction energetics. For the time being, the interaction of the particle with the support is neglected. While these interactions are important for understanding the conductance of electrons away from the active site as well as dissolution and sintering, the weak interaction between the metal and the support suggests that its influence on the intrinsic catalytic behavior may be small. Particle size and structure effects may be examined by using stepped single crystal surface models to probe elementary energetics, however further studies are required to evaluate these effects in a systematic manner. Whereas potential and field effects are directly considered in the model system, we do not explicitly model the polymer electrolyte, nor probe the energetics associated with proton conduction. Additionally, the calculations performed consider only a single adsorbate coverage and a limited model of the dynamic solution phase environment. The absence of each of these effects restricts the ability to directly correlate predicted reaction rates with those observed over a polycrystalline, supported PEMFC anode. The results, however, can be compared with well-designed electrode, single crystal model surface studies and aid in our understanding of the reaction pathways and the kinetics of the elementary processes that occur within the more complex system.

Before describing the development and application of the double-reference method used herein to include the effects of electrode potential within the QM model system, we review some of the previous pioneering efforts in the development and application of QM methods in modeling electrocatalytic systems.

2 Background on the Application of QM Methods to Electrochemical Processes

The developments by Marcus [16] in 1956 greatly advanced the field of electrochemistry and electrocatalysis by enabling a simple yet powerful theoretical framework by which to describe electron transfer reactions. This work has provided the foundation of nearly all subsequent efforts in understanding electron transfer. While a number of these efforts have used Marcus theory together with QM approaches to understand electron transfer at interfaces, for example, between a solvated ion and an electrode in close proximity, there have been very few attempts to couple such an electron-transfer step with the elementary bond-making and bond-breaking steps important for electrocatalysis [17]. Anderson developed and applied Atom-Superposition and Electron-Delocalization Molecular Orbital theory (ASED-MO), a tight-binding QM approach that resulted in some of the first major steps in modeling the chemical transformations in electrocatalytic systems as a function of potential [18, 19]. The models relied on the association of the position of the d-band of the electrocatalyst with the applied potential. The model was later modified to move from a surface description of the reactivity to describe the reactivity of electrodes based on reactive centers whereby the potential of the system was described instead by the ionization potential/electron affinity of the system undergoing oxidation/reduction, respectively [20]. More recently they replaced the qualitative ASED-MO approach with more accurate ab initio QM calculations and have used this approach to follow the various elementary kinetics for simultaneous bond-breaking and electron transfer processes [21].

Unfortunately the extension to systems containing >10 atoms is hindered by the collapse of the ionization potential of the reaction center to the work function of the electrode. It is therefore difficult to establish the same straight-forward relationship between electrocatalytic transition states and the applied potential. Since the metal is modeled as a one or two atom cluster, it cannot explore changes in metal surface structure or composition. In addition, the limitations in the use of small clusters to represent the electronic structure of a metal surface are well known.

A second contemporary approach to the modeling of electrocatalytic processes, particularly those involving coupled proton and electron transfer steps (i.e., A–H $\rightarrow$ A* + H^+ + e^-), is to ignore the effect of the potential on the interfacial chemistry and instead build it strictly into the thermodynamics of the coupled proton–electron transfer. The assumption here is that the electron transfer can be treated separately and that the potential only influences the electron transfer process. This approach has been used to examine the dissociation of water on electrode surfaces [22], as well as to describe O_2 reduction on platinum electrodes [23]. Comparison to methods which more rigorously incorporate electric field effects at the interface, and the electrochemical potential at the metal solution interface (the approach adopted in

this paper), has shown this simple approach to be quite successful in computing electrocatalytic thermodynamics for systems in which the reactant and product state do not show marked differences in the dipole at the metal solution interface. Under these conditions, the electrochemical environment polarizes both the reactant and product states in a very similar way and thus result in only small perturbations to reaction processes occurring at the solution/metal interface of an electrocatalytic system [24]. However, this method is limited in its ability to consider elementary processes in which variations in the interfacial electric field will significantly alter the electronic structure of the adsorbed species. In addition, it is unclear how this approach could be used to analyze the kinetics of systems where electron transfer is important in the actual bond making or bond breaking step.

More recently, ab initio molecular dynamics (AIMD) simulations have been adopted to investigate reaction mechanisms at charged interfaces [25–27]. Several groups, for example, have examined the initial reaction of methanol dehydrogenation over platinum. Problems arise, however, concerning sufficient time-sampling in ab initio MD simulations. In addition, AIMD simulations are carried out in a canonical form whereby the number of electrons and number of atoms is conserved; therefore the electrochemical potential is changing as the electronic structure of the interfacial environment is updated. Additionally, in most of the reported AIMD studies, the potential at which the simulations are performed is not quantified, and often significant amounts of charge are added to motivate electrochemical reactions to occur on the time scale of the AIMD simulation, causing the electrode potential to be well outside the range of the actual electrocatalytic systems.

Herein, we describe an approach developed to model electrochemical and electrocatalytic systems that maintains a constant potential across the electrochemical double layer at the water/metal interface. The metal is treated using a periodic slab model of the electrode, which thus captures the "metallic" nature of the surface. The polarization of the double layer environment is simulated via the introduction of distributed charge and counter-charge to the unit cell. Charge-based models for simulating electrochemistry have typically been challenged by the difficulty in relating charges to electrochemical potentials. We relate the work-function of the periodic slab to the applied potential, as has been well described in classical electrochemical theory. In the following sections we describe the salient points of the method in some detail and its application to elementary processes occurring at fuel cell electrodes to establish the influence of potential.

3 Computational Methods

In an electrochemical system, chemical reactions ultimately lead to development of an electric field or an electrochemical potential at the aqueous metal interface. The field or potential at the electrode–electrolyte interface subsequently affects the stability of adsorbed reactants, transition states, and products, thereby altering the elementary electrocatalytic reaction energies. Herein, the electronic structure of the metal–water interface is simulated using ab initio density functional theory (DFT) calculations. All of the calculations reported were carried out using a periodic plane wave representation of the electronic structure within the Vienna ab initio Simulation Package (VASP) developed by Kresse and Hafner [28–30]. The calculations were performed within the generalized gradient approximation to determine the exchange and correlation energies. Ultrasoft pseudopotentials were employed to describe electron–ion interactions [31]. The metal surface was modeled using super cells comprised of between 3 and 5 metal layers. The center layer of the slab was held fixed at the bulk-phase positions while the outer layers were allowed to relax. Tests comparing 3 and 5 layer metal slabs found little change on the structural or potential-dependent behavior of water [32]. Water molecules were placed between the two metal layers in an ice-like structure in order to simulate the solution environment. The surface metal layers, the adsorbates, and the aqueous interface were optimized for all the structures explored. Further details concerning the specific k-points, cell size, and exchange-correlation functionals employed in the DFT calculations can be found in our previous papers [33, 34]. To reference the potential at the aqueous metal interface and maintain a constant potential between reactants and products, we use an approach that we developed previously and have termed the double reference approach. We only present some of the important features of the approach here and refer the interested reader to the details reported in Refs. [35, 36].

Ideally, the electrochemical double-layer could be modeled by directly including the electrode, the charge-compensating electrolyte and the explicit solution phase water molecules to more fully establish the electronic structure of the electrified aqueous/metal interface. The inclusion of an appropriate concentration of supporting electrolyte and statistical sampling of the various configurations of ion and solvent should produce an accurate description of the electrochemical double-layer within the electronic structure calculation. For example, the addition of a sodium atom near the interface will polarize the interface because the electron affinity of the metal is greater than the sodium cation, thereby attracting electrons

to the metal surface and creating the electrochemical double-layer. The size of the simulation cell, however, limits this approach of direct addition of supporting electrolyte. First, the inclusion of the supporting electrolyte within a small unit cell would lead to unusually high concentrations and thus makes it difficult to establish a sufficient solvation shell about the ion. Second, tuning of the electrode potential in this manner is extremely difficult, as variations require altering the concentration and position of the ions in the cell. This will again require computationally prohibitive unit cell sizes. Furthermore, the comparison of system energies at varying potential would be difficult as the number and types of atoms included in the cell would vary.

The double-reference method instead polarizes the metal–water interface by altering the number of electrons included in the simulation cell. Within a periodic unit cell, the electrode surface is represented as a two-dimensional slab of metal atoms. Water molecules are then included in between the repeating metal slabs, as illustrated in Fig. 2. As the Fermi-level of the metal–water interface is bracketed by filled and unfilled electron levels located on the metal, altering the number of electrons in the unit cell results in a charging of the electrode surface. The requirement of charge neutrality within the periodic unit cell is then met by the addition of a homogeneous background charge. This creates an electric field across the metal–water interface. Though the charge-compensating background charge is unphysical, the environment that it creates at the interface is nearly identical to that created by explicit inclusion of ions along the Helmholtz plane [36]. The adsorption behavior and surface reactivity of the interfacial water as well as any surface adsorbates are then altered as the result of the variation of the potential across the interface. The periodic representation of the metal surface allows for continuous variability in the charge added to the unit cell and therefore the tunability of the electrode potential and the interfacial electric field. Fractional numbers of electrons in the periodic cell simply represent whole charges over a larger number of repeated cells.

Though the representation of the electrochemical double-layer in terms of separated electrode and counter charges is intuitive, the virtue of the double-reference method is in the establishment of an internal reference potential and the ability to determine a system energy that is independent of the changing number of electrons within the unit cell. More detailed derivations and discussions of the assumptions of these methods were previously reported [36]. The electrode potential generated for a given system charge is determined by first referencing the uncharged system potential to the potential of an electron in vacuum. This is done by inserting a vacuum layer in the center of

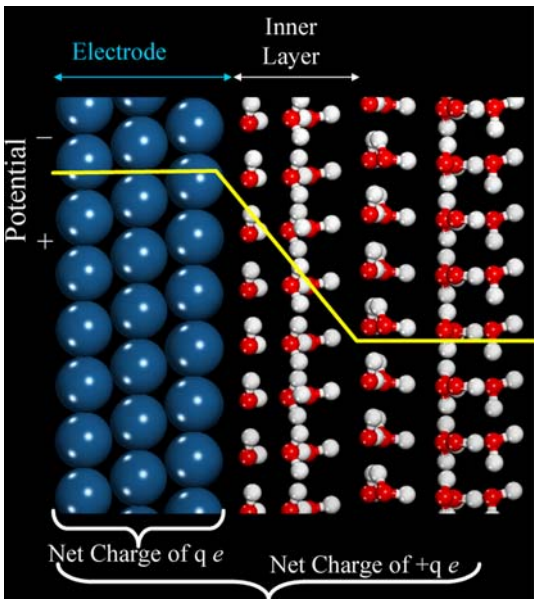

Fig. 2 Illustration of the periodic unit cell employed with the double-reference method to determine the potential dependence of a system free energy. Water molecules are placed between slabs of metal in the unit cell. The electrochemical double-layer is polarized by adding or subtracting electrons from the unit cell. This charge segregates to the electrode surface and a homogeneous background charge is added across the unit cell. The double-reference method then allows for the determination of the electrode potential referenced to the potential of an electron in vacuum and a system free energy independent of the changing charge. Water molecules at the interface can be replaced with reactants or products of an electrocatalytic elementary reaction step, enabling the determination of potential dependent reaction energies

the unit cell. Once the electrode potential of the uncharged system is determined, the potential at the center of the water layer is used as a second reference potential. This potential is assumed to remain constant as the system charge is altered, providing a reference point for the charged-system electrode potential that can then be "double-referenced" to the vacuum potential. The potential of the electrode relative to vacuum (Φ_{vac}), as a function of the system charge q, is then referenced to the potential of a normal hydrogen electrode (Φ_{NHE}) by Eq. 1 [37]:

$$\Phi_{NHE}(q) = -4.8 - \Phi_{vac}(q) \quad (1)$$

All of the potential values reported herein are with reference to the normal hydrogen electrode (NHE).

The total energy of each system must subsequently be corrected for the interaction of the system with the added background charge as well as for the difference in the number of electrons in the charged system. The correction term is added to the total energy calculated at each charge. This correction term is calculated from the vacuum referenced potential (Φ_{vac}) and the volume averaged electrostatic potential of the unit cell, $<\phi>$, as

$$E_{\text{correction}} = \Phi_{\text{vac}} q_e + \int_0^{q_e} < \phi > \mathrm{d}Q \quad (2)$$

where q_e represents the charge added to the unit cell and Q represents the integration variable. The first correction term in Eq. 2 corrects for the change in the number of electrons in the system whereas the second term removes the energy of interaction with the background charge. Therefore, for a given system consisting of the electrode surface, adsorbates, and solution, a series of calculations is performed to determine the optimal structure and energy as a function of potential. Entropic terms can then be added to generate a series of points for the system free energy versus potential, $G(\Phi_{\text{NHE}})$. If the solvation environment remains constant between two systems, such as a reactant and product state of an elementary reaction step, then the difference between the potential dependence of the free energy of the two systems represents the reaction free energy of the elementary step:

$$\Delta G_{\text{reaction}}\ (\Phi_{\text{NHE}}) = G_{\text{product}}\ (\Phi_{\text{NHE}}) - G_{\text{reactant}}\ (\Phi_{\text{NHE}}) \quad (3)$$

This approach explicitly assumes that a single, static solvent structure can produce reaction energies consistent with the dynamic average structure of a macroscopic system. This approximation can be validated by considering multiple solvent structures, or, alternatively, the same cell configuration, potential-reference method, and energy corrections can be employed within a molecular dynamics simulation of the interface. Therefore, the method can be scaled to include variations in structure thus enabling larger systems to be examined as available computational resources increase. However, as water at the metal interface is known to take on an ice-like structure [17], the approximation of a locally optimized, ice-like solvent layer about the adsorbate provides a first approximation to generate relative energies of species adsorbed at the electrode surface.

Within a PEMFC or DMFC, redox elementary steps either produce or consume a proton + electron pair. Due to the limited size of the unit cell employed, the inclusion of a proton in the unit cell creates: (1) a pH discontinuity during the reaction, and (2) an unrealistically low pH (pH < 0). Additionally, it is difficult to develop an appropriate solvation shell about the proton in the unit cell. For these reasons, systems that result in the formation of protons and electrons are treated by defining a bulk continuum reference. The protons or electrons removed from the reaction system are then stored in this continuum reference. The energies to carry out these processes are then calculated by standard thermodynamic steps and subsequently added as a correction to the total free energy. The energy of the proton and electron pair is determined through referencing to the normal hydrogen electrode in a manner similar to that used by Nørskov et al. [23]. This method takes advantage of the equality of the free energy of a gas phase hydrogen molecule with that of a proton and an electron at 0 V (NHE). As the proton generated is taken to have diffused outside the electrochemical double layer, its energy remains constant with potential and only the free energy of the electron must be corrected for the varying potential of the half cell. Therefore, the free energy of a proton and an electron as a function of potential is given as

$$G_{\text{proton+electron}} = G_{1/2\text{hydrogen(gas)}} - e\Phi_{\text{NHE}} \quad (4)$$

where e represents the elementary electron charge. Because the normal hydrogen electrode is defined at a pH of 0, the reaction free energies reported here are given at pH 0, though reaction free energies at different pH values are easily determined by correcting the free energy of the proton in the continuum reference, as is illustrated in a subsequent section.

We have previously considered and tested a number of the approximations made within the application of the double-reference method. The validation of the potential and reaction energies determined with the choice as to the number of metal layers in the slab representation [32] and size of the water layer was performed [38]. Herein, we describe the application of this method to the potential dependence of various different elementary chemical processes occurring at a fuel cell electrode. We first use the approach to examine and compare the electrochemical activation of water over various metal electrode surfaces. We subsequently describe its application to electrocatalysis and illustrate its ability to explain the potential dependence of the products of methanol oxidation by examining the relative reaction energies of initial C–H versus O–H bond activation. The extension to the calculation of potential dependent activation barriers is illustrated by examining the influence of alloying Pt with Ru on the barriers for the oxidation of carbon monoxide to CO_2. Finally, we demonstrate the initial application of this approach in generating design criterion for improved anode compositions for the direct methanol fuel cell. These ideas are subsequently used to screen various different alloy surfaces for improved activity.

4 Results and Discussion

4.1 Electrocatalysis of the H_2O Dissociation Reaction on Pd, Cu, Ni, and Pt Electrodes

Many electrochemical reactions of interest, in terms of practical applicability and fundamental science, are carried out in aqueous solutions. The fundamental interactions

between water and an electrode surface are therefore quite important. It is instructive then to consider the activation of H_2O over an electrode surface as a function of potential before moving to more complicated electrocatalytic reactions.

There is a great wealth of information on the adsorption of water, the surface structures that form and its potential reactivity over well-defined metal substrates that has been established in recent years from single crystal surface science experiments as well as theory and simulation [39, 40]. Much of our current understanding of aqueous water over metals derives from fundamental studies carried out in the vapor phase. There are, however, a number of important differences that can result in significant changes when these reactions are carried out in solution. Dielectric screening, polarization and hydrogen bonding provided by the aqueous medium can all enhance charge and electron transfer processes at the interface, and thus promote reactions that proceed via more polar transition states. We have shown previously that the solution phase can significantly enhance metal catalyzed surface processes and in some cases even open up new reaction channels [41, 42]. Following on these efforts, Filhol and Neurock constructed a model of H_2O over Pd(111) based on simulated annealing of water over the model electrode surface [35]. The resulting structure, shown if Fig. 3, is comprised of a hexagonal bilayer near the surface which repeats into the solution thus taking on a hexagonal ice-like network throughout the nano-dimensioned periodic simulation cell. While this is in part due to the necessity for adopting periodic boundary conditions, it is also a reflection of the observations made both of UHV water-close-packed-metal interfaces [43], and those established from numerous simulations and integral analyses of the electrochemical interface performed over the past few decades [17].

Filhol and Neurock varied the charge on the electrode surface in order to observe the systematic changes in water structure, bond-topology and the electrochemical potential drop occurring throughout the model water-Pd(111) system [35]. Water dissociated at two points along the phase diagram. The first was at a potential of 500 mV which corresponds to the phase transition of water to solution phase hydroxyl intermediates and an adsorbed hydride layer. The second transition occurred at a potential of around 1,100 mV where water reacts to form hydronium ions and an adsorbed hydroxyl phase. Experiments suggest that, under similar conditions, the transitions from the surface-hydride to the surface-water phase and the surface-water to the surface hydroxide phase occur at 0.4 V and 0.7–0.9 V, respectively. The reactions were shown to be irreversible upon a reversal of the charge due to the changes in the solvation shell environment that occur. Variations from the theoretical predictions are likely due to

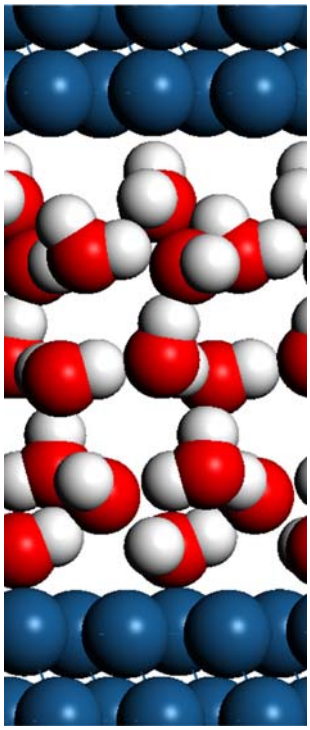

Fig. 3 The ice-like hexagonal structure of water sandwiched between the model electrode slabs as utilized as a first-order model for the electrochemical interface

the small, finite size of the periodic model: for these calculations a $\sqrt{3} \times \sqrt{3}$ unit cell was used, constraining a high periodicity of the adsorbate and solvation lattice, artificially raising the potential required to make the transition thermodynamically viable. Furthermore, the activation of water released protons into the lattice, and, in this early version of the model, no correction was made for the high acidity produced (a ratio of 1 H_3O^+ to 6 water molecules). We now discuss corrections made to this dilemma in more recent work.

While these were some of the first simulations to fully treat a metal electrode, an aqueous solution and the reactions between them in a purely first principle QM framework, various approximations had to be made. We examine them here and consider their validity. One of the most important approximations was the assumption that the solution could be modeled as an optimized water layer at 0 K without introducing the influence of solution dynamics. Some of our previous results were found to be insensitive to the water dynamics at the surface. While there are dynamic fluctuations of the water molecules, they do not appear to affect the overall reaction energies. They can, however, influence the system potential, especially in comparing an ice-like layer where the dipole moments for all of the water molecules are oriented with an aqueous solution. Second, the formation of OH^- (aq) and H^+(aq) ions from the activation of adsorbed water leads to a pH

discontinuity within the small simulation cell. It would be of greater advantage in the determination of the electrode thermodynamics to consider a grand canonical system where the H^+ and OH^- ions that form can exchange with an external reservoir. Finally, the simulation cell adopted here has a $\sqrt{3} \times \sqrt{3}$ periodicity. This size of the surface may not be large enough to fully capture the influence of coadsorbed water which can act to stabilize the intermediates and products. The approach taken by Filhol was later extended by Taylor et al. [44] over Cu(111), and used to examine a broader range of potentials. A number of these issues were removed by ultimately using a much larger 3×3 unit cell as well as external reservoirs to solvate the H^+/OH^- species that form. The results of this study showed that, as the potential was increased from the potential of zero charge, water was activated to form surface hydroxide intermediates followed by a surface oxide layer that formed at further increases of the potential. At high enough potentials, the adsorbed oxygen and the surface Cu atoms exchange places ultimately leading to the dissolution of solvated Cu^{2+} ions and a passivating Cu_2O overlayer atop the Cu(111) surface [44].

Subsequent simulations for the electrochemical activation of water over the metal adopted a grand-canonical ensemble, in which the energy of the protons used/produced was incorporated by adding the term μN to the product system, where μ is determined from the energy of a solvated proton estimated from quantum mechanics and tabulated experimental ionization and solvation energies. In this way the pH is maintained at a constant neutral value throughout the simulations, and variations in pH can be considered by simply adding NRT $\ln[H^+]$ to μN. We have applied this approach to the activation of water over different model metal substrates including Cu(111) [44], Ni(111) [32], and Pt(111) [24]. Figure 4a, b, for example, presents the regions of temperature/pH phase-space over which H_2O and its dissociation products are stable over the ideal (111) surfaces of Cu and Ni respectively. The agreement with the limited in situ STM observations of OH overlayer formation over single crystal surfaces is quite reasonable but not within electrochemical accuracy, which is on the order of 10 mV or less. For example, the water to hydroxyl transition over Ni(111) has been observed using in situ STM [45] and found to coincide with the point (pH 3, −0.16 V). This point lies within the potential region of surface coverage by hydroxyl predicted in this study. The potential for complete surface oxidation appears at +0.09 V (at pH of 3) which is within the predicted region of oxygen coverage on the Ni(111) surface. Thus while the domain predictions are correct, the transition points are not precise when compared to experiment. Future iterations of this model, involving ensemble averaging and extended multiscale models, will likely help improve this agreement.

The thermodynamic changes were also related to the geometric changes that occurred. For example, the bond length between the oxygen on water and the Cu(111) and Ni(111) surfaces decreases as the surfaces become more positively charged. The adsorbed hydrogen, on the other hand, demonstrates an opposite effect as we move to more cathodic potentials. This results in a weaker interaction of hydrogen on Ni(111) yet a stronger interaction for hydrogen on Cu(111). The strong chemisorption of atomic oxygen to the metal surface can act to significantly weaken the local metal–metal bonds. At higher potentials and more positive surface change densities, this can enhance the

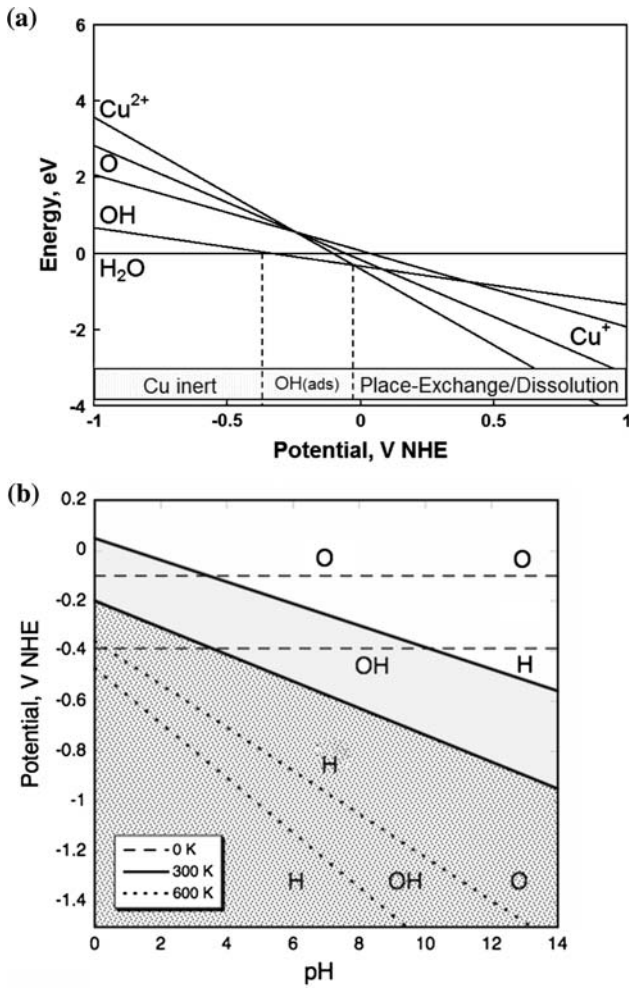

Fig. 4 Phase diagrams indicating the regions of H, OH, and H_2O stability at the electrochemical interface on (**a**) Cu(111) at pH 13 and 300 K and (**b**) Ni(111) over a range of pH. Thermodynamic quantities at 300 and 600 K are derived from ab initio data (at 0 K) using standard statistical mechanical approximations. Shading represents demarcations of surface adsorption phase-space at 300 K, according to the labeling of each region (O, OH, H). The PW91 GGA exchange-correlation form was used to solve the electronic structure for Cu and Pt, whereas RPBE was used for Ni. In all cases a 3×3 lattice was used and 24 water molecules were in the unit cell (23 H_2O + 1 OH after activation)

place-exchange between the adsorbed oxygen and surface metal atoms and potentially lead to the synchronous onset of oxide formation and metal dissolution.

The activation of water can be greatly influenced by the presence of other surface intermediates. We have shown, for example, that the coadsorption of CO with water on Pt(111) can significantly modify the response of local Pt atoms to the activation of water. The coadsorption of CO and water on sites directly next to one another shifts the equilibrium potential for activation of $H_2O \leftrightarrow OH$ from 0.79 V (in the absence of CO) to 1.29 V (in the presence of CO). Analysis of the charge distribution and the adsorption geometries suggests that the electron withdrawing/electron donating aspects of OH and CO donation compete to modify their mutual adsorption thermodynamics and thereby shift the equilibrium potential between OH and H_2O adsorption [46].

The achievements made in theory and simulation have made it possible to describe the qualitative electrochemical reactivity of water over metal substrates and the semi-quantitative prediction of thermodynamic and geometric parameters. These results indicated that the application to electrocatalytic reactions was not only feasible, but a promising way to explore the sensitivity of reaction geometries, thermodynamics and potentially kinetics, to the electrochemical environment, thereby providing a framework for the determination of potential dependent redox reaction energy paths.

4.2 Electrocatalytic Mechanisms—Methanol and CO Oxidation Over Pt and Pt–Ru Alloys

The potential dependent reaction energies for a sequence of elementary reaction paths involved in the electrooxidation of methanol to CO were modeled using the double reference method [33]. The overall reaction energies for the possible C–H and O–H bond breaking processes were calculated as a function of potential to establish which paths would be likely at different operating potentials. At most of the potentials of interest, the primary path involves the activation of the methanol C–H bond to form an adsorbed hydroxymethyl intermediate. The calculations suggest that the Hydroxymethyl intermediate oxidizes to form hydroxy methylene on the surface. This species subsequently forms an adsorbed formyl that oxidizes to produce an adsorbed CO species.

At potentials greater than 0.5 V, the calculated results indicate that the activation of the O–H bond becomes more competitive with C–H bond activation. The resulting reaction paths, along with the overall reaction energy diagram for methanol dehydrogenation at 0.5 V over Pt(111), are illustrated in Fig. 5. The reaction energy for dehydrogenation of methanol to methoxide (O–H cleavage) becomes more favorable as the potential becomes more positive. Assuming that the reaction barrier for each step scales with the reaction energy via an Evans–Polanyi relationship, the relative rate of O–H cleavage would be expected to increase at more positive potentials. The results shown in Fig. 5 indicate that the major path at 0.5 V (depicted in bold and blue) still proceeds through the formation of the surface hydroxyl methyl intermediate which ultimately goes on to form CO. The minor path leads to the formation of the formaldehyde intermediate as shown in the path depicted in italics and red in Fig. 5.

The work described thus far has used the double-reference method to analyze overall reaction energies for different elementary reaction steps. We recently extended this method to calculate potential dependent activation barriers [34, 47].

The primary path for methanol oxidation produces carbon monoxide as a reaction intermediate. The strong adsorption of the CO surface intermediate that forms inhibits further surface reactions and thus limits the performance of DMFC anodes [5, 7]. Because of its critical importance, we examined the elementary steps as well as the intrinsic kinetics for CO oxidation using the double-reference method. We calculated the potential dependent reaction barriers for the coupling of adsorbed carbon monoxide with hydroxyl or oxygen species over the Pt(111) surface [34]. Transition states were identified using the climbing image nudged elastic band method [48−50] in which the saddle point along the reaction coordinate between two species is identified. This method requires the charge of the unit cell to be continuous between reactants and products. As the charge that produces a given electrode potential differs with different species adsorbed, the electrode potential is subject to change between reactants and products, thereby making the assignment of a potential to the transition state difficult. In the coupling of adsorbed CO and OH or O intermediates, however, the potential change between reactants and products is small and the assignment of the potential of the transition state to that of the reactant state introduces only a slight approximation. The barrier for the coupling of a carbon monoxide surface intermediate with an adsorbed hydroxyl species was found to be significantly lower than the barrier associated with the coupling of CO with adsorbed oxygen, as illustrated in Fig. 6.

This barrier, put in context of the entire reaction mechanism, illustrates that the majority of CO oxidation proceeds through coupling with the hydroxyl surface intermediate which helps to confirm that adsorbed OH acts as the oxidant. The barrier for coupling adsorbed CO and OH over the Pt(111) surface decreases with increasing potential. The barrier at 0.5 V is close to 0.55 eV and drops

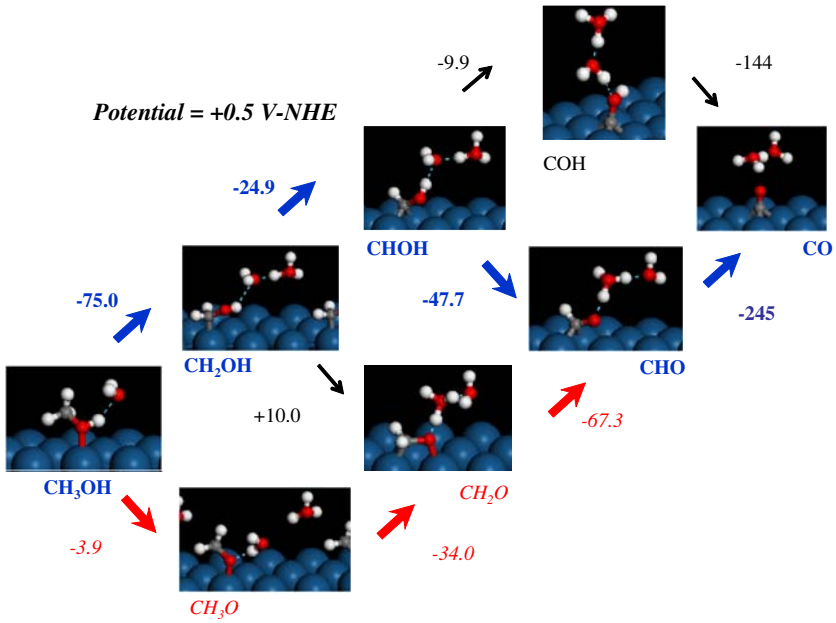

Fig. 5 DFT-calculated elementary step reaction energies for the dehydrogenation of methanol to CO over Pt(111) at a potential of 0.5 V-NHE. Reaction energies are given in kJ mol^{-1}. The lowest energy path to formation of CO through the hydroxymethyl intermediate is shown in bold and blue. The minor path leading to the formation of a formaldehyde intermediate is shown in italics and red. All energies were computed with 3 × 3 surface cells and the RPBE form of the GGA exchange-correlation functional

to approximately 0.25 eV at 1.5 V. This decrease occurs due to greater stabilization of charge separation at the transition state, as solvation of the hydroxyl species polarizes the transition state. This polarization is substantially larger than for coupling with an adsorbed O atom due to the lesser degree of solvation provided by the single aqueous layer structure examined. The increased rate constant for this reaction step contributes together with a higher surface coverage of adsorbed hydroxyl intermediates to increase the rate of CO oxidation at higher potentials.

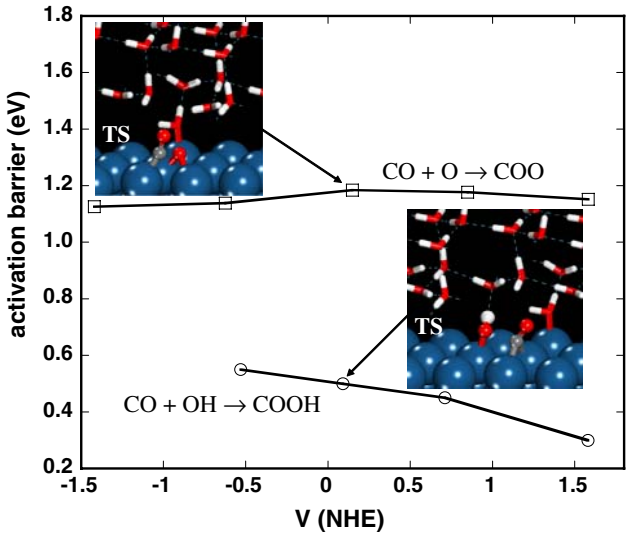

Fig. 6 Potential dependence of activation barriers for the coupling of adsorbed carbon monoxide with adsorbed oxygen or hydroxyl species. The barrier for coupling with the hydroxyl species is substantially lower at all potentials, and decreases at more positive potentials. This decrease is partly responsible for the increased rate of CO oxidation at more positive potentials. All energies were computed with 3 × 3 surface cells and the RPBE form of the GGA exchange-correlation functional

In addition to the analysis of CO oxidation over pure Pt(111), the reaction energies involved in the oxidation of CO over different Pt–Ru alloy surfaces were also examined [47]. Platinum–ruthenium alloys demonstrate enhanced CO tolerance as anode materials for both hydrogen as well as direct methanol fuel cells. While this enhancement has been attributed to both ligand and bifunctional effects, the direct determination of the dependence of oxidation rates on alloy structure remains a challenge. Figure 7 illustrates reaction energy diagrams, determined using the double-reference method, for the oxidation of CO at 0.9 V over pure Pt(111), Pt_2Ru_1 over Pt(111), Pt over Ru(0001), and Pt_2Ru_1 over Ru(0001). Compared to the pure Pt surface, the inclusion of Ru atoms in the surface reduces the reaction energy for water oxidation to form surface hydroxyl species (Fig. 7b). The increase of the CO* + OH* coupling barrier, however, reduces the rate of CO oxidation, indicating that a pure bifunctional effect it not solely responsible for the increased rate (Fig. 7b). A Ru substrate under the Pt surface slightly increases the endothermicity of water oxidation, but reduces the barrier for the CO + OH coupling reaction significantly thus allowing for significantly improved CO oxidation rates (Fig. 7c).

The combination of the PtRu surface alloy and the pseudomorphic Pt_{ML}/Ru overlayer generates the mixed $PtRu_{ML}$/Ru overlayer system shown in Fig. 7d. The mixed $PtRu_{ML}$/Ru overlayer results in a decreased reaction energy for water activation and a coupling barrier lower than the same overlayer on a Pt substrate (Fig. 7b), indicating that both bifunctional and ligand effects may combine to

enhance the rate of CO oxidation. This mixed overlayer system illustrates the difficulty in assigning the increase in the CO oxidation rate quantitatively to either of the bifunctional or ligand effects, as an increased rate at 0.9 V would be due to a higher coverage of hydroxyl species on the surface Ru atoms (bifunctional effects) despite the higher barrier to the coupling step. However, if the electronic structure of the surface were not altered by the substrate Ru atoms (ligand effect), the stronger binding of CO and OH to the surface would significantly increase the barrier for the CO* + OH* coupling and thereby decrease the oxidation rate.

4.3 Toward the Design of DMFC Anode Catalysts

The double-reference method has proven to be quite useful in analyzing potential dependent reaction energies as well as activation barriers and thus elucidating electrocatalytic reaction mechanisms. In this section, we explore how changes in the catalyst composition can alter the elementary reaction energetics for different elementary steps occurring at a DMFC anode. The ideality of the model surfaces and interfaces examined make the quantitative comparison of the theoretical results with any specific experiment a challenge. However, if we assume that the changes in the metal and alloy composition have a significant influence, we can use the approach to compare different catalyst compositions and thus recommend possible surface compositions and structures that may result in improved electrode performance as compared to a pure Pt electrode. Regretfully, the need to determine the electronic structure of the water layer and to consider multiple system charges to probe the potential dependence requires substantial computational resources which can limit the systems that can be analyzed using the double reference method. With the key reaction steps that determine reactivity and selectivity at different potentials of interest determined, the catalytic performance can be established through the use of more approximate models. For example, the performance of an alloy catalyst for methanol oxidation over a range of potentials between 0 and 0.8 V-NHE can be evaluated by examining its ability to carry out important elementary steps such as the activation of both the C–H and O–H bonds of methanol, the O–H bond activation of water, the coupling of coadsorbed CO and OH, and the desorption of CO, as outlined in the Table 1.

The reaction energies for the relevant reaction steps or adsorption energies were calculated for a series of different bimetallic surface alloys using only the gas-phase/metal interface model and constant system charges between reactant and product states. The potential dependence of reaction energies was subsequently determined by relating the overall surface reaction energies calculated in the vapor phase to those under electrochemical conditions through a linear expansion of the Nernst equation as follows:

$$\Delta G(U) = \Delta G(U_0) + \Delta_q F(U - U_0) \quad (5)$$

where U is the electrochemical potential and U_0 is the potential of zero charge.

This approach is similar to that developed by Nørskov [23, 51] and holds quite well provided that the second order term in the free energy expansion, which concerns the changes in the capacitance, is small. The results from this

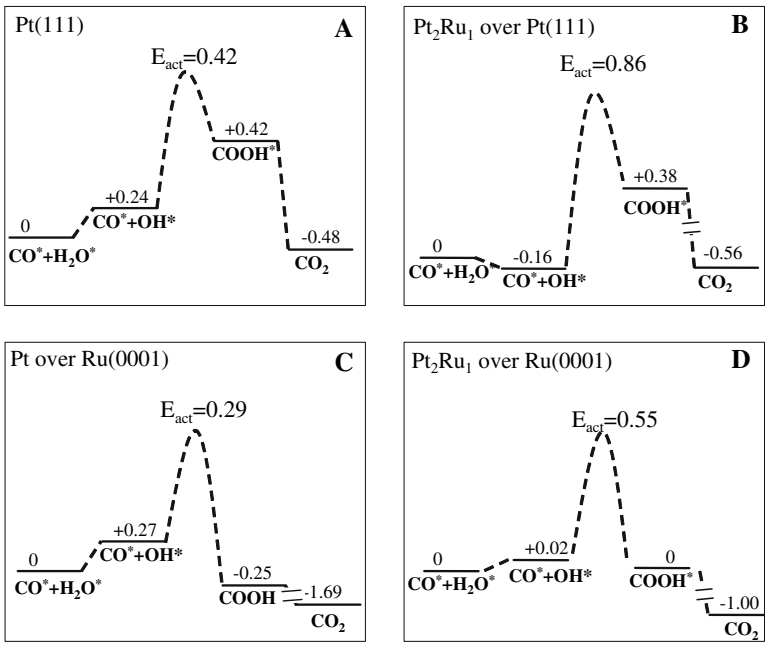

Fig. 7 Reaction energy diagrams for CO oxidation over Pt and Pt-Ru alloy surfaces. (**a**) Pt(111), (**b**) Pt_2Ru_1 monolayer over a Pt(111) substrate, (**c**) Pt monolayer over a Ru(0001) substrate, and (**d**) Pt_2Ru_1 monolayer over a Ru(0001) substrate. All energies were computed with 3 × 3 surface cells and the RPBE form of the GGA exchange-correlation functional

Table 1 Design criteria of an improved methanol fuel cell anode and reaction energy measurements used to evaluate performance

DMFC anode property	Elementary energy measurement
Preferentially break C–H versus O–H bonds of the methanol reactant, leading to a greater selectivity for oxidation through carbon monoxide rather than partial oxidation to formaldehyde	ΔE_{rxn} $CH_3OH \rightarrow CH_2OH + H^+ + e^-$ compared to ΔE_{rxn} $CH_3OH \rightarrow CH_3O + H^+ + e^-$
Provide for a rate of methanol oxidation to CO similar to that of pure Pt	ΔE_{rxn} $CH_3OH \rightarrow CH_2OH + H^+ + e^-$
Reduce the binding energy of CO with respect to pure Pt	ΔE_{ads} $CO_{gas} \rightarrow CO_{ads}$
Provide sites for the activation of water to adsorbed hydroxyl species, while balancing the reaction energy for coupling of CO and OH	ΔE_{rxn} $H_2O \rightarrow OH + H^+ + e^-$ ΔE_{rxn} $CO + OH \rightarrow CO_{2\ gas} + H^+ + e^-$
Remain stable as a surface ensemble under electrode operating conditions	Not currently evaluated

approach have been shown to match those from the double-reference method [24] well provided that there is not a significant change in the dipole moment between the reactant and the product state at the surface nor significant long-range interactions with the solvent environment. As only comparisons between different compositions of catalyst were desired, the solvation and dipole–field interaction terms were not added to the calculation of reaction energies. The overall reaction energies presented are given at 0.5 V, chosen as a suitable reference for comparing the performance of various compositions. The results in Table 2 summarize many of the initial compositions considered to probe the performance of DMFC anodes. The values given in italics indicate potentially improved performance of a given composition with respect to the pure Pt(111) surface. Note that improved performance with respect to all of these measures may not be necessary in order to improve the performance of the DMFC anode. For example, the Pt monolayer over Ru(0001) does not show an improved ability to activate water, however, the previous section illustrated that it may show enhanced CO oxidation rates. These results represent an initial attempt to identify candidates that may show improved methanol oxidation kinetics which can be further pursued through more detailed theoretical calculations or experimental studies.

Despite the consideration of various overlayer, surface alloy, and bulk alloy compositions, we were not successful in locating a binary alloy system with significant promise for better performance compared to the Pt–Ru alloy. One encouraging system based on elementary reaction energetics was that for a monolayer of Ir over a Cu(111) substrate. This system shows an enhancement in both C–H bond activation and water activation as measured by their increased overall reaction exothermicity, as well as a slightly weakened CO binding with respect to pure Pt(111) or Ir(111). However, this system likely fails the final criteria, the stability of the overlayer system, which was not evaluated herein. While Pt–Ru alloys show encouraging cooperative effects whether the Ru is in the surface or subsurface, including Cu in an Ir(111) surface would likely lead to a decrease in performance of the DMFC anode, as the CO binding would increase with respect to pure Ir(111).

On moving to ternary alloys, however, the identification of promising anode compositions was more successful. As an example, the ternary PtRuAu surface alloy supported on the Ru(0001) surface is included in Table 2. This surface, while slightly less favorable for dehydrogenation than Pt alone, significantly increases CO tolerance with respect to Pt or Pt–Ru alloys The CO binding energy is reduced and the CO* + OH* coupling reaction is substantially more exothermic compared to pure Pt(111) or a Pt ML over Ru(0001). This would likely lead to a significantly reduced barrier to the important CO* + OH* coupling step, identified as an important parameter for CO tolerance in the previous section. Finally, both Pt and Au may be expected to segregate to the surface of this ternary alloy system, though investigation of this factor was not completed. Though these results are far from conclusive on the improvement this composition may bring to anode performance, they provide an example of how ab initio QM methods can be used to provide fundamental understanding of the electrochemical system and aid in suggesting new electrode compositions for improved catalytic performance. A complicating factor not considered in our calculations is the possibility that the individual metals may prefer to phase segregate in the surface layer. Experimental investigations are currently underway to evaluate whether this ternary alloy can be synthesized in a manner that provides for the successful trade-off of dehydrogenation activity for increased CO tolerance to improve the DMFC anode performance.

5 Summary

The double-reference method described herein provides a formalism by which ab initio QM calculations can be used to probe the elementary reaction energetics that dictate the performance of electrode materials. The approach was also

Table 2 Reaction energies of key elementary steps for methanol oxidation over pure metal and alloy surfaces

Surface	CH_3OH $CH_2OH + H^+ + e$	CH_3OH $CH_3O + H^+ + e$	H_2O $OH + H^+ + e$	CO_{gas} CO_{ads}	$CO + OH$ $CO_{2\ gas} + H^+ + e$
Pt(111)	−0.27	+0.63	+0.58	−2.00	−0.07
Pt ML over Ru(0001)	−0.07	*+0.65*	+0.73	*−1.27*	*−1.16*
Pt ML over Pd(111)	*−0.34*	*+0.82*	+0.67	−2.01	*−0.24*
Pt ML over Au(111)	*−0.33*	+0.40	+0.71	−2.34	+0.14
Cu ML over Zn(0001)	+0.62	−0.55	+0.84	*−0.85*	*−1.57*
Au ML over Cd(0001)	+0.45	+0.40	*+0.35*	*−0.36*	*−1.73*
Ir(111)	−0.11	+0.22	*+0.27*	*−1.94*	+0.23
Ir ML over Cu(111)	*−0.64*	*+0.68*	*−0.13*	*−1.90*	+0.29
Ru_1Pt_2 over Pt(111)	−0.20	+0.59	*+0.42*	−2.20	+0.73
Pt_1Ru_2 over Ru(0001)	−0.01	+0.06	*+0.25*	*−1.77*	+0.16
Sn_1Pt_2 over Pt(111)	+0.12	*+0.94*	*+0.30*	*−1.19*	*−0.62*
Ni_1Pt_2 over Pt(111)	−0.26	+0.11	+0.64	*−1.99*	+0.05
Ag_1Pt_2 over Pt(111)	−0.20	+0.52	*+0.43*	*−1.76*	*−0.29*
Pt_1Au_2 over Au(111)	+0.02	*+1.00*	+0.72	*−1.59*	*−0.67*
Cu_1Ir_2 over Ir(111)	*−0.29*	+0.23	*+0.13*	−2.21	+0.74
Ir_1Cu_2 over Cu(111)	−0.08	+0.48	*+0.26*	−2.28	+0.50
PtAuRu over Ru(0001)	+0.34	+0.33	*+0.39*	*−1.03*	*−0.70*

Note: Overlayer and surface alloy compositions were considered to compare performance with the pure Pt surface. All oxidation reaction energies are given at 0.5 V-NHE, as detailed in the text. Values in italics indicate possible improved performance for that reaction step compared to pure Pt(111). For surface alloys, CO was assumed to adsorb on the site most active for methanol dehydrogenation, for example, atop of the Pt atom in alloys including Pt. All calculations utilized a 3 × 3 surface cell and the PW91 GGA functional for the exchange and correlation energy

used to simulate the electrochemical activation of water over various metal surfaces, thus helping to validate the ability of these methods to provide reasonable quantitative information for the potential dependent behavior of different surface redox reactions. The double reference method was subsequently used to follow the reaction energies for the dehydrogenation steps involved in methanol oxidation over Pt(111) and provide mechanistic insights into the factors which control the primary pathways that lead to carbon monoxide and secondary paths responsible for formaldehyde production at higher potentials. Further determination of potential-dependent reaction energies and activation barriers for the elementary steps of CO oxidation over Pt–Ru alloys illustrated the role of alloy structure in enabling both ligand and bifunctional effects to increase the rate of CO oxidation. Finally, the insights gained from the application of the double-reference method were used to probe the design of improved anode compositions for methanol oxidation. Future work will extend the method to establish a more complete model of the reaction environment including the influence of surface structure and composition, coverage effects, metal-support effects and the influence of the polymer electrolyte.

Acknowledgements This work was supported by the Army Research Office—MURI grant (DAAD19-03-1-0169) for fuel cell research. Computational resources at the Environmental Molecular Sciences Laboratory at Pacific Northwest National Laboratory were used, in part, to complete this research as well as computing resources at the U.S. Army Research Laboratory Major Shared Resource Center. The authors thank Dr. Sally Wasileski, Dr. Jean-Sebastian Filhol, and Dr. Andrzej Wieckowski for their contributions to this research effort.

References

1. Donitz W (1998) Int J Hydrogen Energy 23:611
2. Wasmus S, Kuver A (1999) J Electroanal Chem 461:14
3. Haile SM (2003) Acta Materialia 51:5981
4. Bagotzky VS, Osetrova NV, Skundin AM (2003) Russ J Electrochem 39:919
5. Dillon R, Srinivasan S, Arico AS, Antonucci V (2004) J Power Sources 127:112
6. Gasteiger HA, Kocha SS, Sompalli B, Wagner FT (2005) Appl Catal B 56:9
7. Jusys Z, Behm RJ (2001) J Phys Chem B 105:10874
8. Roth C, Benker N, Buhrmester T, Mazurek M, Loster M, Fuess H, Koningsberger DC, Ramaker DE (2005) J Am Chem Soc 127:14607
9. Gasteiger HA, Marković N, Ross PN Jr, Cairns EJ (1993) J Phys Chem 97:12020
10. Gasteiger HA, Marković N, Ross PN Jr, Cairns EJ (1994) J Phys Chem 98:617
11. Gasteiger HA, Marković NM, Ross PN Jr (1995) J Phys Chem 99:8290
12. Jusys Z, Kaiser J, Behm RJ (2002) Electrochim Acta 47:3693
13. de Mongeot FB, Scherer M, Gleich B, Kopatzki E, Behm RJ (1998) Surf Sci 411:249
14. Miki A, Ye S, Osawa M (2002) Chem Comm 1500
15. Waszczuk P, Lu G-Q, Wieckowski A, Lu C, Rice C, Masel RI (2002) Electrochim Acta 47:3637

16. Marcus RA (1956) J Chem Phys 24:966
17. Guidelli R, Schmickler W (2000) Electrochim Acta 45:2317
18. Anderson AB, Awad MK (1985) J Am Chem Soc 107:7854
19. Anderson AB, Ray NK (1982) J Phys Chem 86:488
20. Anderson AB (2003) Electrochim Acta 48:3743
21. Anderson AB, Cai Y, Sidik RA, Kang DB (2005) J Electroanal Chem 580:17
22. Rossmeisl J, Logadottir A, Nørskov JK (2005) Chem Phys 319:178
23. Nørskov JK, Rossmeisl J, Logadottir A, Lindqvist L, Kitchin JR, Bligaard T, Jónsson H (2004) J Phys Chem B 108:17886
24. Rossmeisl J, Nørskov JK, Taylor CD, Janik MJ, Neurock M (2006) J Phys Chem B 110:21833
25. Okamoto Y, Sugino O, Mochizuki Y, Ikeshoji T, Morikawa Y (2003) Chem Phys Lett 377:236
26. Mattson TR, Paddison SJ (2003) Surf Sci 544:L697
27. Hartnig C, Spohr E (2005) Chem Phys 319:185
28. Kresse G, Furthmüller J (1996) Comput Mater Sci 6:15
29. Kresse G, Furthmüller J (1996) Phys Rev B 54:11169
30. Kresse G, Hafner J (1993) Phys Rev B 47:558
31. Vanderbilt D (1990) Phys Rev B 41:7892
32. Taylor CD, Kelly RG, Neurock M (2006) J Electrochem Soc 153:E207
33. Cao D, Lu G-Q, Wieckowski A, Wasileski SA, Neurock M (2005) J Phys Chem B 109:11622
34. Janik MJ, Neurock M (2007) Electrochim Acta 52:5517
35. Filhol JS, Neurock M (2006) Angew Chem Int Ed 45:402
36. Taylor CD, Wasileski SA, Filhol JS, Neurock M (2006) Phys Rev B 73:165402
37. Reiss H, Heller A (1985) J Phys Chem 89:4207
38. Taylor CD, Kelly RG, Neurock M (2007) J Electrochem Soc 154:F55
39. Henderson MA (2002) Surf Sci Rep 46:1
40. Marković NM, Ross PN Jr (2002) Surf Sci Rep 45:117
41. Desai SK, Pallassana V, Neurock M (2001) J Phys Chem B 105:9171
42. Desai SK, Neurock M (2003) Phys Rev B 68:075420
43. Doering DL, Madey TE (1982) Surf Sci 123:305
44. Taylor CD, Kelly RG, Neurock M (2007) Phys Rev B submitted
45. Suzuki T, Yamada T, Itaya K (1996) J Phys Chem 100:8954
46. Taylor CD, Janik MJ, Neurock M, Kelly RG (2007) Mol Sim 33:429
47. Janik MJ, Neurock M, in preparation
48. Henkelman G, Jónsson H (2000) J Chem Phys 113:9978
49. Henkelman G, Uberuaga BP, Jónsson H (2000) J Chem Phys 113:9901
50. Mills G, Jónsson H, Schenter GK (1995) Surf Sci 324:305
51. Liu P, Logadottir A, Nørskov JK (2003) Electrochim Acta 48:3731